Nanohole arrays in chemical analysis: manufacturing methods and applications

Jean-François Masson,*[abc] Marie-Pier Murray-Méthot[a] and Ludovic S. Live[a]

Received 1st February 2010, Accepted 7th March 2010
First published as an Advance Article on the web 31st March 2010
DOI: 10.1039/c0an00053a

Since the last decade, nanohole arrays have emerged from an interesting optical phenomenon to the development of applications in photophysical studies, photovoltaics and as a sensing template for chemical and biological analyses. Numerous methodologies have been designed to manufacture nanohole arrays, including the use of focus ion beam milling, soft-imprint lithography, colloidal lithography and, more recently, modified nanosphere lithography (NSL). With NSL or colloidal lithography, the experimental conditions control the density of the nanosphere mask and, thus, the aspect of the nanohole arrays. Low surface coverage of the nanosphere mask produces disordered nanoholes. Ordered nanohole arrays are obtained with a densely packed nanosphere mask in combination with electrochemical deposition of the metal, glancing angle deposition (GLAD) or etching of the nanospheres prior to metal deposition. A review of these methodologies is presented here with an emphasis on the optical properties of nanoholes interesting in analytical chemistry. In particular, applications of these novel plasmonic materials will be demonstrated as substrates for a localized surface plasmon resonance (LSPR), Surface Plasmon Resonance (SPR), surface enhanced Raman spectroscopy (SERS), and in electrochemistry with nano-patterned electrodes.

1. Introduction

In 1998, Ebbesen *et al.* reported that enhanced transmission is observed when light impinges on a metallic film with sub-wavelength nanoholes.[1] This enhanced light transmission is anomalously high for specific wavelengths, attributed to the different plasmonic modes in the nanohole arrays. Theory and general optical properties will not be discussed here as they were the object of reviews elsewhere.[2,3] Interesting physico-chemical properties can be exploited from this optical phenomenon, which renders these materials useful in numerous fields. In particular, nanohole arrays could find applications in optics, probably as optical bandpass filters due to the selective wavelength transmission of light.[4] The wavelength at which the enhanced

[a]*Département de Chimie, Université de Montréal, C.P. 6128 Succ. Centre-Ville, Montréal, QC, Canada H3C 3J7. E-mail: jf.masson@umontreal.ca; Fax: +1-514-343-7586; Tel: +1-514-343-7342*
[b]*Centre for Self-Assembled Chemical Structures (CSACS), McGill University, Montréal, QC, Canada H3A 2K6*
[c]*Centre for Biorecognition and Biosensors (CBB), McGill University, Montréal, QC, Canada H3A 2B4*

Jean-François Masson

Jean-François Masson is currently an assistant professor of Chemistry at Université de Montréal. His field of expertise covers multiple aspects of sensing, such as plasmonic materials, surface chemistry and detection in biofluids. He is a member of the Centre for Self-Assembled Chemical Structures (CSACS) and the Centre for Biorecognition and Biosensors (CBB).

Ludovic S. Live (left) and Marie-Pier Murray-Méthot (right)

Ludovic S. Live and Marie-Pier Murray-Méthot are, respectively, PhD and MSc students in the Chemistry Department at Université de Montréal. Their research work focuses on biosensing with micro plasmonic materials and nanohole arrays.

transmission occurs shifts with refractive index of a thin layer of solution in contact with the nanoholes.[5] This sensitivity to refractive index of nanohole arrays is useful in biosensing.[6] Surface Plasmon Resonance (SPR) with a Kretschmann configuration is an established technique using refractive index sensitivity for bioanalyses.[7] Ring resonators are emerging in chemical analysis, also based on refractive index sensitivity.[8,9] Moreover, an enhanced electrical field is generated when incident light excites an active plasmonic mode of the nanoholes.[10] This enhanced electrical field can be exploited for surface enhanced Raman scattering (SERS).[11] Lastly, the continuous network of metal in nanohole arrays exhibits electrical conductance. Therefore, nanohole arrays can also be used as semi-transparent electrodes for photovoltaic applications.[12,13] These numerous applications highlight the importance of nanohole arrays in numerous fields.

Most nanohole arrays reported to date are of cylindrical (circular) hole shape. Although theoretical models for the optical response of nanohole arrays does not include the effect of the hole diameter and shape, it was recently reported that arrays of nanoholes with circular, triangular and square nanohole shape exhibit significantly different optical properties.[14] However, the optimal hole shape for SPR sensors remains to be determined. In SERS, surfaces with an irregular shape generally increase the Raman signal of surface-bound molecules. This was demonstrated with nanohole arrays of double-hole structure.[15,16] Hence, nanohole arrays to be used in Raman spectroscopy should exploit this advantage.

The fabrication of an ordered nanohole arrays has been first reported in 1995 by Masuda and Fukuda.[17] They accomplished the fabrication of nanohole arrays using a replication process of an anodized alumina structure. Since then, numerous strategies have been developed to manufacture nanohole arrays. These techniques can be categorized as serial for milling techniques and parallel for lithographic techniques. Among these methodologies, focus ion beam (FIB) milling has demonstrated excellent reproducibility, and control on the size and shape of nanoholes.[18–21] Hence, FIB has been of great use in theoretical studies of the optical phenomenon and for the development of biosensors. However, FIB is costly to run and requires long milling times to manufacture arrays larger than 100 × 100 μm. These limitations of the fabrication process may prevent the use of FIB for massively parallel production of nanohole arrays.[22] These drawbacks are partially alleviated with lithographic techniques such as soft embossing with a mask prepared using e-beam lithography.[23–27] Briefly, this approach uses an imprinting mask that can be printed on a surface numerous times to increase the fabrication rate and the area covered with nanoholes. The holes created by this imprinting mask are thereafter covered with metal to generate the nanohole arrays. For more information, a detailed review explaining soft embossing has been published elsewhere.[28] Another approach uses phase-shifting photolithography, etching, electron beam deposition and lifting (PEEL).[29] Removable cylindrical posts are fabricated using this technique, which leads to nanohole arrays after lift off of the nanoposts. These techniques could provide the reproducibility and tunability in size and shape required for massively parallel fabrication of nanohole arrays. These lithographic techniques require a different mask/templates to fabricate nanohole arrays with different physical aspects. However, there is currently a need for the systematic study of nanohole arrays with various shapes or sizes. This makes photolithographic techniques time consuming and difficult to use for the optimization of the optical properties of nanohole arrays.

Modified nanosphere lithography (NSL) techniques were recently developed to provide the tunability, rapid fabrication and low manufacturing cost required to develop nanohole arrays with optimal plasmonic properties. Disordered nanoholes can be manufactured using colloidal lithography,[30] while ordered nanohole arrays are obtained from NSL in combination with electrochemical deposition,[31] ion-polishing,[32] plasma treatment[32–40] and glancing angle deposition (GLAD).[38,41,42] An overview of the fabrication process and numerous applications of nanohole arrays prepared using modified nanosphere lithographic techniques are discussed in this Minireview.

2. Disordered nanoholes

Nanoholes using colloidal lithography as a preparation methodology were first introduced as disordered nanoholes. The deposition of charged nanospheres to a surface yields a sub-monolayer coverage.[30] In this method, a silicon wafer surface is modified with a positively charged layer. Negatively charged polystyrene beads are deposited on the positively charged surface. The fractional coverage is typically below 0.45 due to electrostatic interactions between polystyrene beads limiting the packing density of the spheres at the surface. These electrostatic interactions are shielded with increasing ionic strength. Ionic strength, adsorption time and sphere concentration control the number of nanoholes per unit area on the surface. For large salt concentrations, aggregation between polymer nanospheres is possible, thus ionic strength control is essential to obtain isolated nanoholes. Deposition of a metal layer on this mask followed by desorption of the mask leads to disordered nanoholes[30] (Fig. 1A).

The disordered nanosphere mask is also the premise for the fabrication of different structures. Among others, hole-mask colloidal lithography exploits the disordered nanohole arrays as a mask to fabricate a variety of structures such as nanodiscs, nanocones, pairs of nanodiscs, and embedded nanodiscs.[43]

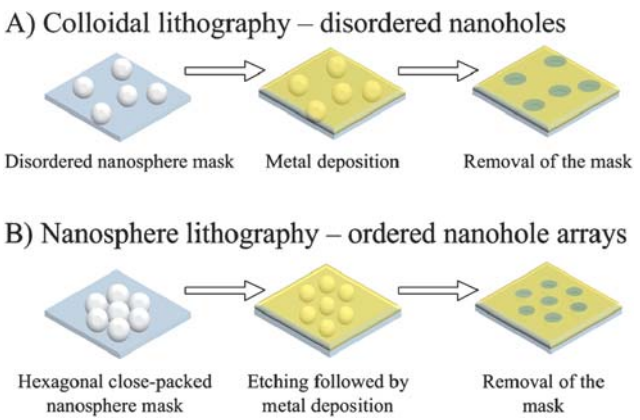

Fig. 1 Schematic representation for the fabrication of (A) disordered nanoholes with colloidal lithography and (B) ordered nanohole arrays using modified NSL.

Nanorings were also fabricated using a diluted nanosphere mask by rotating the sample in the deposition chamber.[44] Another variation of colloidal lithography yields nanorings and nanocrescents with oblique deposition of the metal film, followed by etching at a normal angle of the metal film.[45–50] Suspended Si_3N_4 nanohole arrays were fabricated on a Si wafer by depositing disordered nanoholes, followed by a selective etching of the silicon wafer.[51] Oxygen plasma controls the sphere size while at the surface providing a technique to tune the diameter of the nanohole. This is especially useful when low surface coverage is desired with small nanoholes, as the smaller spheres do not show the same adsorption behavior to surfaces.[30] Depositing the metal layer in an atmosphere containing 20% oxygen can decrease the nanosphere size while depositing the metal layer.[52] This last concept of controlling the size of polymer nanospheres while immobilized on a surface is essential to fabricate ordered nanohole arrays.

3. Ordered nanohole arrays

This section will emphasize on strategies for the fabrication of ordered nanohole arrays by modifying conventional NSL. Nanospheres can be deposited on a surface in a close-packed hexagonal arrangement using neutral nanospheres.[53,54] This type of NSL has been popularized to fabricate nanotriangle arrays used in localized surface plasmon resonance (LSPR) and SERS for more than a decade.[55–57] NSL is advantageous in terms of cost, size of the area produced (mm^2 to cm^2) with few defects and is simple to implement. However, the close hexagonal arrangement of the nanospheres does not provide the proper spacing between nanospheres to deposit a metal film and obtain deep nanoholes of cylindrical shape, as obtained with focus ion beam milling, soft embossing and photolithographic techniques. Maintaining the crystalline order of the nanosphere mask is also advantageous, as it allows for applications where a photonic crystal is needed and a greater density of nanoholes can be obtained in a biosensor format.

3.1 Nanohole arrays by electrochemical deposition of a metal mask

Electrochemical deposition of metal onto a surface modified with an NSL mask proved to be adequate to form ordered nanohole arrays.[31] The electrochemically deposited metal film fills the gap created within adjacent spheres and the surface, except for the contact points between the nanospheres and the surface. This results in nanoholes of hemispherical cross-section. The periodicity of the nanohole is dictated by the diameter of the nanospheres, and the depth is controlled with the metal deposition time, while the nanohole diameter cannot be controlled. The simplicity of this methodology makes it easy to implement.

3.2 Nanohole arrays by glancing angle deposition

One technique to fabricate ordered nanohole arrays involves the deposition of the metal layer at an oblique angle with a planetary stage to rotate the nanosphere mask in the deposition chamber.[38] The combination of rotation and deposition at an angle of 27° allowed the formation of nanohole arrays. This technique results in nanoholes of hexagonal shape. However, the depth of the nanoholes is limited to less than 20 nm, due to the deposition process. Deposition at a 45° angle with GLAD yielded nanowires.[38,42] Nonetheless, the nanohole arrays exhibited plasmonic properties, which could be tuned according to the depth of the nanoholes and deposition angle.[38]

3.3 Nanohole arrays by etching an NSL mask

Alternatively, several groups have recently reported similar techniques using a gas plasma to create ordered nanohole arrays. Thereby, the nanosphere mask can be etched prior to the deposition of the metal film.[58] This etching step creates a gap between adjacent spheres, which results in an ordered, non-close-packed nanosphere mask (Fig. 1B). In one example, a CF_4:O_2 plasma was used to ion-polish polystyrene nanospheres and silica.[32,59] The spheres of an initial 300 nm diameter were etched from 300 to <100 nm.[32] Ion-polishing does not decrease significantly the sphere diameter for the first 360 s, which was explained as a consequence of the top-down etching of the nanospheres. Thereby, nanohole arrays with identical periodicity were prepared with hole sizes of decreasing diameter. This technique shows the simple tuning of the nanohole diameter with etching of the NSL mask.

Polystyrene beads were etched in a pure oxygen plasma to decrease the size of the nanospheres.[58] It was reported that the etch rate is also non-linear with time,[58,60] similar to the CF_4:O_2 plasma. For most reported techniques, the etch rate is approximately 1 nm s^{-1}.[32,35,58,60] However, it is still important to measure the diameter with surface characterization techniques, such as SEM, to calibrate the etch rate of the nanospheres with individual etching systems. Fig. 2 shows SEM images at different steps of the nanohole arrays preparation method. Some roughness is introduced on the nanosphere, but general ordering of the NSL mask is maintained.[60] Annealing the spheres subsequently to the etching step mitigates this inconvenience.[60] Alternatively, switching from a reactive ion etching system to an inductively coupled plasma can also limit the roughness of the nanospheres.[61] Another methodology controls the size, shape and smoothness of the etch nanospheres with low-temperature (−150 °C) etching.[62] Modified nanosphere lithography controls the periodicity with the initial diameter of the nanospheres, the diameter of the hole with the etch time and the depth of the nanohole from the thickness of metal deposited.

Variation on reactive ion etching with oxygen includes etching of silica beads to fabricate nanohole arrays.[35,39,63,64] Nanopillars are formed using the silica nanospheres. These nanopillars act as a template for the formation of the nanohole arrays.[63] Also, etching spheres in an oxygen plasma is not limited to nanospheres and has also been applied to microspheres.[64–67] Microhole arrays are therefore produced and were used in an SPR system with a Kretschmann configuration.[66] Lastly, a mixture of Ar and O_2 was used to etch polystyrene nanospheres with similar results as etching with pure O_2.[36]

Typically, round or elliptical nanoholes are obtained with NSL combined with reactive ion etching. Depositing metal at a normal angle from the surface leads to round nanoholes. Tilting the sample in the metal deposition chamber creates a shadow effect on the deposition resulting in elliptical nanoholes. Non-spherical nanoholes are fabricated using pre-heating

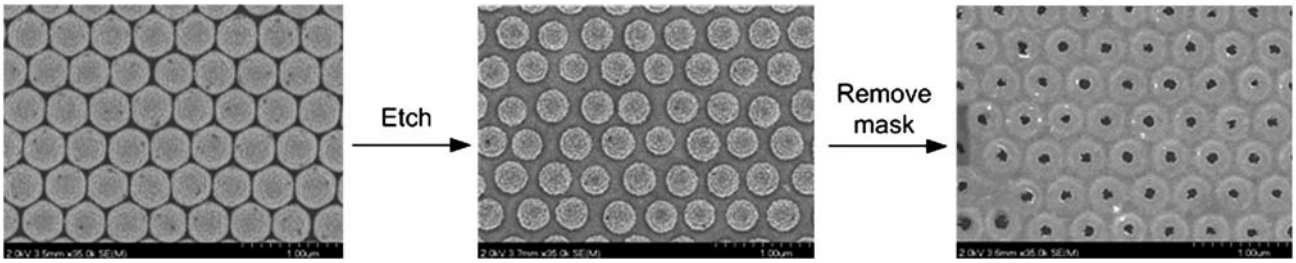

Fig. 2 SEM images of the nanosphere mask (left), after etching with oxygen plasma (center) and resulting in metallized nanohole arrays after removal of the mask (right). The long axis of the images is 3.6 μm.

of a single layer or double layers of polystyrene beads.[34] The template of nanoholes generated with modified NSL was used to fabricate Si nanowires.[68] Moreover, filling the nanoholes with a material, followed by removal of the nanohole template also yields nanowires. Thereby, the nanowires are normal from the surface, as they are connected from the terminal end and have the long edge extending away from the surface. A similar technique has been applied for the fabrication of nanowires of molecularly imprinted polymers.[69]

3.4 Analytical and optical properties of nanohole arrays

An important application of metallic nanohole arrays in analytical chemistry uses refractive index sensitivity to construct biosensors. The analytical parameters of importance include the sensitivity, the spectral position of the plasmonic band, the sensitivity to monolayer formation and the resolution of refractive index measurements. Thus, the study of these optical properties is essential in assessing the potential of nanohole arrays as biosensors.

The transition between localized surface plasmons (SPs) on nanoparticles and propagating SPs on nanohole arrays was observed with etching an NSL mask for increasing times to fabricate triangle and nanohole arrays. The optical response switched from a localized SPR signal for triangles to the extended surface plasmon observed in ordered nanohole arrays.[37] The typical LSPR absorption band was observed for unetched samples, which initially red shifted with increasing etch time. For short etch times, triangles of increasing edge lengths are obtained. This increases the aspect ratio (edge length/height) of the triangles. Hence, the red shift was similar to the one reported for arrays of triangles with increasing aspect ratio.[55] At the transition point between triangle and nanohole arrays, the LSPR absorption band disappeared (from the 450–800 nm spectral range), and a new plasmonic band was visible at approximately 480 nm. This demonstrated that plasma etching the NSL mask provides a simple method for tuning of the hole diameter and the optical properties.

Correlation of the optical properties for nanohole arrays prepared by modified NSL and other techniques has not been directly reported. However, for nanohole arrays with 450 nm periodicity, an extensive amount of work has been accomplished for ordered Au nanohole arrays prepared with various techniques.[33,36,38,40] These nanohole arrays were fabricated with modified NSL combined with plasma etching. An example of the transmission spectrum obtained with ordered nanohole arrays is shown in Fig. 3. The plasmonic wavelength in ordered nanohole arrays can be calculated from eqn (1) for square arrays of nanoholes and from eqn (2) for hexagonal arrays of nanoholes:[70]

$$\lambda_{SPR}(i,j) = \sqrt{\frac{\varepsilon_m \varepsilon_s}{\varepsilon_m + \varepsilon_s}} \frac{P}{\sqrt{i^2 + j^2}} \quad (1)$$

$$\lambda_{SPR}(i,j) = \sqrt{\frac{\varepsilon_m \varepsilon_s}{\varepsilon_m + \varepsilon_s}} \frac{P}{\sqrt{\frac{4}{3}(i^2 + ij + j^2)}} \quad (2)$$

where the variables are the periodicity of the array (P), the dielectric constants of the metal (ε_m) and of the solution (ε_s) in contact with the nanohole arrays, and $\lambda_{SPR}(i,j)$ is the plasmonic wavelength for the Bragg resonance orders i,j. Moreover, finite-difference time-domain (FDTD) calculation closely matches the experimental spectrum for nanohole arrays.[36] The plasmonic peak at the lower wavelength in Fig. 3 was correlated to the solution/nanohole interface and the peak at higher wavelength was attributed to the glass/nanohole interface.[36,71] Accordingly, the sensitivity to the solution refractive index of the lower wavelength peak is 226 nm/RIU, while the sensitivity for the glass/nanohole plasmonic peak is an order of magnitude lower.[38] The sensitivity to the refractive index is slightly lower compared to FIB-manufactured nanoholes (333 nm/RIU).[5] However, the FIB-milled nanoholes are a square array of 150 nm holes compared to the hexagonal array of 320 nm holes obtained with

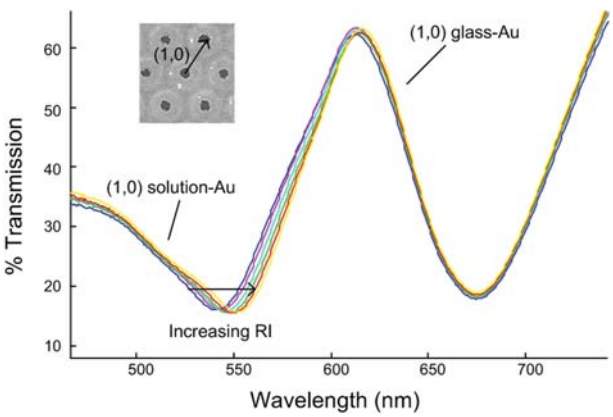

Fig. 3 Spectrum of ordered nanohole arrays acquired in transmission; the periodicity is 450 nm. The (1,0) solution-Au peak is sensitive to the refractive index (RI) while the (1,0) glass-Au peak does not change with increasing refractive index.

modified nanosphere lithography. The sensitivity difference is likely to be due to these different physical parameters of the nanohole arrays.

Sensitivity to the formation of an organic thiol monolayer was measured with ordered nanohole arrays. The wavelength shift was on the order of 1–2 nm.[5,38] This is significantly lower than LSPR on triangle arrays (up to 40 nm).[55] The response to monolayer formation on disordered nanoholes with low hole density (single nanohole) is quite large, with up to 10–15 nm for pentadecanethiol.[72] However, disordered nanoholes of higher hole density yield a significantly smaller shift upon formation of a monolayer. The shift for a short chain alkanethiol is negative with disordered nanoholes of high density, while for longer chains the shift is on the order of a few nanometers.[72] Hence, the shift observed for disordered nanoholes of high density is similar to ordered nanohole arrays.

Another important analytical parameter to consider is the refractive index resolution. Improving RI resolution generally results in better detection limits. Typically, an RI resolution on the order of 10^{-4} RIU is obtained for ordered nanohole arrays.[38] It will need to be improved in comparison to conventional SPR, for which the RI resolution is on the order of 10^{-6} to 10^{-7} RIU.[7] Data analysis methodologies are one solution to improve the signal-to-noise (S/N) ratio. Reducing the shot noise provides better S/N, combined with calculating the centroid wavelength of the plasmonic response in nanohole arrays.[73] Alternatively, nanohole arrays of greater sensitivity and with sharp plasmonic bands will also improve the RI resolution.

4. Applications

4.1 Plasmonic-based biosensors

In order to construct a biosensor based on nanohole plasmonic materials, the surface of the metal is chemically-derived with thiols bearing chemical functionality. These thiols are then modified with molecular recognition elements such as antibodies, DNA, or enzymes among others. To date, among nanohole prepared using nanosphere/colloidal lithography, only disordered nanoholes have been used in a biosensor format. A supported lipid bilayer was deposited on disordered nanoholes.[74] This lipid bilayer remains mobile at the surface as demonstrated with fluorescence recovery after photobleaching (FRAP). Nonetheless, the diffusion rate was slower than on unpatterned thin film.[75] The cavity of the nanohole has been used to probe lipid-membrane biorecognition events. Each nanohole is used as a well to locally probe binding events. Recently, a single vesicle per nanohole was immobilized on the supported lipid membrane.[76] This sensing template was used to detect complementary DNA strands.

Ordered nanohole arrays prepared using FIB or soft embossing techniques have been used in a biosensor format. Several biosensing demonstration with nanohole arrays used bovine serum albumin (BSA) as the model system.[20,77–80] These articles reported that the adsorption of BSA induced a shift of the plasmonic wavelength of the nanohole arrays biosensor. A specific sensor for immunoglobulin G (IgG) was constructed using nanohole arrays.[81] The working range of this sensor was in the nM, with a detection limit of 0.4 nM. In another example, the detection of streptavidin was reported using a biotinylated monolayer.[6] Analysis of the response provides insight on the number of molecules probed. It was estimated that approximately 2000 molecules/nanohole are probed, with an array of 30×30 nanoholes. A flow-through format of nanoholes reduces the response time, as measured with antibody binding.[82] Other examples include glutathione S-transferase (GST) monitored in the nM concentration range[24] and a cortisol derivative bound to the nanohole arrays was detected using a monoclonal antibody and a secondary antibody tagged with a Au nanoparticle.[27] These examples highlights the numerous possibilities of the nanohole arrays biosensors.

4.2 Nanoholes integrated into quartz-crystal microbalance (QCM)

Plasmonic sensing using disordered nanoholes was combined with QCM detection.[74,83] The disordered nanoholes are fabricated on the sensing crystal of the QCM. Both techniques are complementary, as nanoholes measure the change of refractive index with a binding event and QCM measures the change in mass caused by the binding event. The different molecular properties measured with each technique causes a different response factor for QCM and plasmonic detection of biomolecules. Thus, when comparing responses between technique, this response factor must be taken into account. Simultaneous detection for neutravidin and IgG was accomplished using LSPR and QCM.[83] This demonstrated the potential of coupling other analytical techniques with nanohole arrays.

4.3 Surface enhanced spectroscopy

SERS is a well-established technique to amplify the Raman response of molecular adsorbates. For a couple decades, substrates manufactured based on NSL have played a major role in the development of SERS.[56] In recent years, nanohole arrays have been reported as a material exhibiting SERS.[84,85] In one example, disordered nanoholes were used to amplify the Raman response of Rhodamine 6G.[11,86] A comparative study of nanohole arrays and Au colloids demonstrated similar SERS intensity[11] (Fig. 4). SERS was performed on disordered nanoholes prepared with 50 nm[11] or 140 nm spheres[86] and an excitation laser of 632.8 nm. An ordered nanohole array was also used to amplify the Raman spectrum of rhodamine 6G.[87] Recently, the amplification of the Raman response for benzenethiol was compared for a nanohole arrays with flat Ag and Ag film over nanosphere (AgFON) substrates.[36] This last study with benzenethiol reported that the nanohole arrays exhibited a 10–100× increase of the enhancement factor. These studies demonstrate the potential of nanohole arrays in Raman spectroscopy.

Surface plasmon enhanced IR absorption (SEIRA) was reported with micron-size meshes with holes of sub-wavelength diameter.[2,88] The micron periodicity of the hole arrays results in IR excitation of the plasmons. Similarly to SERS, the enhanced electrical field amplifies the IR response of adsorbed molecules.

4.4 Photovoltaics/electrode materials/photophysics

Metallic nanohole arrays are conducting materials, which can be used as an electrode. Recent articles report their use in various

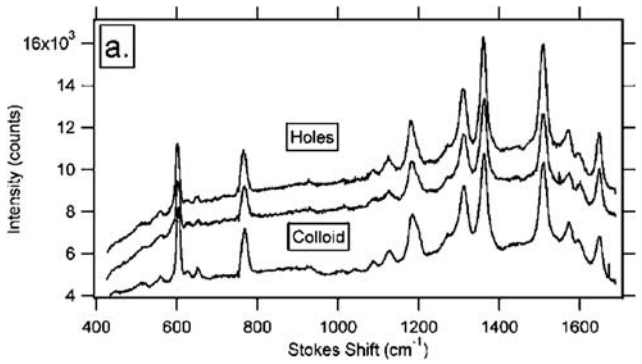

Fig. 4 SERS spectra on disordered nanoholes and on Au colloid. The middle trace for nanoholes and the bottom trace with Au colloids were acquired under the same conditions with 1.4×10^{-6} M rhodamine 6G. (Reproduced with permission from ref. 11. Copyright 2006, Society for Applied Spectroscopy.)

applications. One of these possible applications is the use of the nanohole arrays as semi-transparent electrodes.[13] The nanohole arrays could replace the indium tin oxide (ITO) front electrode in organic photovoltaics. ITO is an expensive material with limited availability. ITO can also migrate out to the organic layer and poison its performance.[13] Porous electrodes such as nanohole arrays have also been investigated for enhancing the sensitivity of electrochemical sensors[12] and the intensity of electrochemiluminescence.[89] The photophysics of pentacene were also studied with the aim of enhanced solar energy conversion.[90] Lastly, nanohole arrays have been integrated into microelectromechanical systems (MEMS).[91,92] It is foreseeable that other applications deriving from the use of nanohole arrays as electrodes will emerge in the next years.

Photophysical studies have been reported to understand some of the underlying principles of nanohole arrays. Disordered nanohole sensors have been used in the study of optically thin gold films.[93] These thin nanohole films exhibited plasmonic properties similar to LSPR substrates. Another study reported that the plasmonic response of the nanohole arrays increased with a thicker overlayer.[94] The wavevector-resolved spectral imaging of nanoholes was accomplished.[95] Thereby, the regions of highest sensitvity of the Brillouin zone are obtained.

5. Conclusions

Nanohole arrays are a recent plasmonic material and most work has been accomplished on manufacturing such structures, characterizing the optical properties, and modeling the optical response. Simple methodologies have been designed to manufacture nanohole arrays with tunable optical and physical properties. The use of NSL is advantageous in terms of cost, time required to prepare the nanohole arrays and reproducibility. Numerous applications of these nanohole plasmonic materials are currently being developed and the next decade should witness significant advances. There is still very few analytical applications that have been reported, but with the simple manufacturing techniques reported recently, this could increase rapidly. Nanohole arrays still need optimization of their analytical properties to achieve their potential for various applications. Modified NSL provides the fabrication methodology to achieve these studies.

References

1 T. W. Ebbesen, H. J. Lezec, H. F. Ghaemi, T. Thio and P. A. Wolff, *Nature*, 1998, **391**, 667.
2 J. V. Coe, J. M. Heer, S. Teeters-Kennedy, H. Tian and K. R. Rodriguez, *Annu. Rev. Phys. Chem.*, 2008, **59**, 179.
3 H. T. Liu and P. Lalanne, *Nature*, 2008, **452**, 728.
4 B. Gauvreau, A. Hassani, M. F. Fehri, A. Kabashin and M. Skorobogatiy, *Opt. Express*, 2007, **15**, 11413.
5 A. De Leebeeck, L. K. S. Kumar, V. de Lange, D. Sinton, R. Gordon and A. G. Brolo, *Anal. Chem.*, 2007, **79**, 4094.
6 J. Ferreira, M. J. L. Santos, M. M. Rahman, A. G. Brolo, R. Gordon, D. Sinton and E. M. Girotto, *J. Am. Chem. Soc.*, 2009, **131**, 436.
7 J. Homola, S. S. Yee and G. Gauglitz, *Sens. Actuators, B*, 1999, **54**, 3.
8 H. Y. Zhu, I. M. White, J. D. Suter, P. S. Dale and X. D. Fan, *Opt. Express*, 2007, **15**, 9139.
9 H. Y. Zhu, I. M. White, J. D. Suter, M. Zourob and X. D. Fan, *Anal. Chem.*, 2007, **79**, 930.
10 S. H. Chang, S. K. Gray and G. C. Schatz, *Opt. Express*, 2005, **13**, 3150.
11 J. T. Bahns, F. N. Yan, D. L. Qiu, R. Wang and L. H. Chen, *Appl. Spectrosc.*, 2006, **60**, 989.
12 T. Lohmuller, U. Muller, S. Breisch, W. Nisch, R. Rudorf, W. Schuhmann, S. Neugebauer, M. Kaczor, S. Linke, S. Lechner, J. Spatz and M. Stelzle, *J. Micromech. Microeng.*, 2008, **18**, 115011.
13 T. H. Reilly, J. van de Lagemaat, R. C. Tenent, A. J. Morfa and K. L. Rowlen, *Appl. Phys. Lett.*, 2008, **92**, 243304.
14 J. H. Kim and P. J. Moyer, *Appl. Phys. Lett.*, 2006, **89**, 121106.
15 L. K. S. Kumar, A. Lesuffleur, M. C. Hughes and R. Gordon, *Appl. Phys. B: Lasers Opt.*, 2006, **84**, 25.
16 A. Lesuffleur, L. K. S. Kumar, A. G. Brolo, K. L. Kavanagh and R. Gordon, *J. Phys. Chem. C*, 2007, **111**, 2347.
17 H. Masuda and K. Fukuda, *Science*, 1995, **268**, 1466.
18 A. G. Brolo, R. Gordon, B. Leathem and K. L. Kavanagh, *Langmuir*, 2004, **20**, 4813.
19 J. Dintinger, I. Robel, P. V. Kamat, C. Genet and T. W. Ebbesen, *Adv. Mater.*, 2006, **18**, 1645.
20 A. Lesuffleur, H. Im, N. C. Lindquist and S. H. Oh, *Appl. Phys. Lett.*, 2007, **90**, 243110.
21 D. Sinton, R. Gordon and A. G. Brolo, *Microfluid. Nanofluid.*, 2008, **4**, 107.
22 A. V. Whitney, B. D. Myers and R. P. Van Duyne, *Nano Lett.*, 2004, **4**, 1507.
23 J. Henzie, J. E. Barton, C. L. Stender and T. W. Odom, *Acc. Chem. Res.*, 2006, **39**, 249.
24 J. Ji, J. G. O'Connell, D. J. D. Carter and D. N. Larson, *Anal. Chem.*, 2008, **80**, 2491.
25 J. H. Kim and P. J. Moyer, *Appl. Phys. Lett.*, 2007, **90**, 131111.
26 E. S. Kwak, J. Henzie, S. H. Chang, S. K. Gray, G. C. Schatz and T. W. Odom, *Nano Lett.*, 2005, **5**, 1963.
27 J. C. Sharpe, J. S. Mitchell, L. Lin, H. Sedoglavich and R. J. Blaikie, *Anal. Chem.*, 2008, **80**, 2244.
28 M. E. Stewart, C. R. Anderton, L. B. Thompson, J. Maria, S. K. Gray, J. A. Rogers and R. G. Nuzzo, *Chem. Rev.*, 2008, **108**, 494.
29 J. Henzie, J. Lee, M. H. Lee, W. Hasan and T. W. Odom, *Annu. Rev. Phys. Chem.*, 2009, **60**, 147.
30 P. Hanarp, D. S. Sutherland, J. Gold and B. Kasemo, *Colloids Surf., A*, 2003, **214**, 23.
31 T. A. Kelf, Y. Sugawara, R. M. Cole, J. J. Baumberg, M. E. Abdelsalam, S. Cintra, S. Mahajan, A. E. Russell and P. N. Bartlett, *Phys. Rev. B: Condens. Matter Mater. Phys.*, 2006, **74**, 245415.
32 Y. B. Zheng, S. J. Wang, A. C. H. Huan and Y. H. Wang, *J. Appl. Phys.*, 2006, **99**, 034308.
33 V. Canpean and S. Astilean, *Mater. Lett.*, 2009, **63**, 2520.
34 C. X. Cong, W. C. Junus, Z. X. Shen and T. Yu, *Nanoscale Res. Lett.*, 2009, **4**, 1324.
35 W. H. Huang, C. H. Sun, W. L. Min, P. Jiang and B. Jiang, *J. Phys. Chem. C*, 2008, **112**, 17586.
36 S. H. Lee, K. C. Bantz, N. C. Lindquist, S. H. Oh and C. L. Haynes, *Langmuir*, 2009, **25**, 13685.
37 W. A. Murray, S. Astilean and W. L. Barnes, *Phys. Rev. B: Condens. Matter Mater. Phys.*, 2004, **69**, 165407.
38 M. P. Murray-Methot, N. Menegazzo and J. F. Masson, *Analyst*, 2008, **133**, 1714.

39 C. H. Sun, W. L. Min and P. Jiang, *Chem. Commun.*, 2008, 3163.
40 V. Canpean and S. Astilean, *Nucl. Instrum. Methods Phys. Res., Sect. B*, 2009, **267**, 397.
41 C. M. Zhou and D. Gall, *Thin Solid Films*, 2007, **516**, 433.
42 M. T. Zin, K. Leong, N. Y. Wong, H. Ma and A. K. Y. Jen, *Nanotechnology*, 2007, **18**, 455301.
43 H. Fredriksson, Y. Alaverdyan, A. Dmitriev, C. Langhammer, D. S. Sutherland, M. Zaech and B. Kasemo, *Adv. Mater.*, 2007, **19**, 4297.
44 X. F. Peng and I. Kamiya, *Nanotechnology*, 2008, **19**, 315303.
45 R. Bukasov and J. S. Shumaker-Parry, *Nano Lett.*, 2007, **7**, 1113.
46 R. Bukasov and J. S. Shumaker-Parry, *Anal. Chem.*, 2009, **81**, 4531.
47 J. S. Shumaker-Parry, H. Rochholz and M. Kreiter, *Adv. Mater.*, 2005, **17**, 2131.
48 L. Y. Wu, B. M. Ross and L. P. Lee, *Nano Lett.*, 2009, **9**, 1956.
49 X. D. Zhou, S. Virasamy, W. Knoll, K. Y. Liu, M. S. Tse and L. W. Yen, *J. Nanosci. Nanotechnol.*, 2008, **8**, 3369.
50 X. D. Zhou, S. Virasawmy, W. Knoll, K. Y. Liu, M. S. Tse and L. W. Yen, *Plasmonics*, 2007, **2**, 217.
51 X. A. Zhang, Z. W. Zhu, C. F. Sun, F. Zhu, Z. Z. Luo, J. W. Yan and B. W. Mao, *Microchim. Acta*, 2009, **167**, 135.
52 X. F. Peng and I. Kamiya, *Appl. Surf. Sci.*, 2009, **255**, 4384.
53 U. C. Fischer and H. P. Zingsheim, *J. Vac. Sci. Technol.*, 1981, **19**, 881.
54 J. C. Hulteen and R. P. Vanduyne, *J. Vac. Sci. Technol., A*, 1995, **13**, 1553.
55 C. L. Haynes and R. P. Van Duyne, *J. Phys. Chem. B*, 2001, **105**, 5599.
56 P. L. Stiles, J. A. Dieringer, N. C. Shah and R. P. Van Duyne, *Annu. Rev. Anal. Chem.*, 2008, **1**, 601.
57 K. A. Willets and R. P. Van Duyne, *Annu. Rev. Phys. Chem.*, 2007, **58**, 267.
58 C. Haginoya, M. Ishibashi and K. Koike, *Appl. Phys. Lett.*, 1997, **71**, 2934.
59 B. J. Y. Tan, C. H. Sow, T. S. Koh, K. C. Chin, A. T. S. Wee and C. K. Ong, *J. Phys. Chem. B*, 2005, **109**, 11100.
60 L. L. Yan, K. Wang, J. S. Wu and L. Ye, *J. Phys. Chem. B*, 2006, **110**, 11241.
61 C. Brombacher, M. Saitner, C. Pfahler, A. Plettl, P. Ziemann, D. Makarov, D. Assmann, M. H. Siekman, L. Abelmann and M. Albrecht, *Nanotechnology*, 2009, **20**, 105304.
62 A. Plettl, F. Enderle, M. Saitner, A. Manzke, C. Pfahler, S. Wiedemann and P. Ziemann, *Adv. Funct. Mater.*, 2009, **19**, 3279.
63 W. Wu, D. Dey, A. Katsnelson, O. G. Memis and H. Mohseni, *J. Vac. Sci. Technol., B*, 2008, **26**, 1745.
64 W. Wu, D. Dey, O. G. Memis, A. Katsnelson and H. Mohseni, *Nanoscale Res. Lett.*, 2008, **3**, 123.
65 C. F. Chau and T. Melvin, *J. Micromech. Microeng.*, 2008, **18**, 064012.
66 L. S. Live and J. F. Masson, *J. Phys. Chem. C*, 2009, **113**, 10052.
67 L. S. Live, M. P. Murray-Methot and J. F. Masson, *J. Phys. Chem. C*, 2009, **113**, 40.
68 K. Q. Peng, M. L. Zhang, A. J. Lu, N. B. Wong, R. Q. Zhang and S. T. Lee, *Appl. Phys. Lett.*, 2007, **90**, 163123.
69 A. V. Linares, F. Vandevelde, J. Pantigny, A. Falcimaigne-Cordin and K. Haupt, *Adv. Funct. Mater.*, 2009, **19**, 1299.
70 T. Thio, H. F. Ghaemi, H. J. Lezec, P. A. Wolff and T. W. Ebbesen, *J. Opt. Soc. Am. B*, 1999, **16**, 1743.
71 J. M. McMahon, J. Henzie, T. W. Odom, G. C. Schatz and S. K. Gray, *Opt. Express*, 2007, **15**, 18119.
72 T. Rindzevicius, Y. Alaverdyan, A. Dahlin, F. Hook, D. S. Sutherland and M. Kall, *Nano Lett.*, 2005, **5**, 2335.
73 A. B. Dahlin, J. O. Tegenfeldt and F. Hook, *Anal. Chem.*, 2006, **78**, 4416.
74 M. P. Jonsson, P. Jonsson and F. Hook, *Anal. Chem.*, 2008, **80**, 7988.
75 A. Dahlin, M. Zach, T. Rindzevicius, M. Kall, D. S. Sutherland and F. Hook, *J. Am. Chem. Soc.*, 2005, **127**, 5043.
76 A. B. Dahlin, M. P. Jonsson and F. Hook, *Adv. Mater.*, 2008, **20**, 1436.
77 G. M. Hwang, L. Pang, E. H. Mullen and Y. Fainman, *IEEE Sens. J.*, 2008, **8**, 2074.
78 V. Malyarchuk, M. E. Stewart, R. G. Nuzzo and J. A. Rogers, *Appl. Phys. Lett.*, 2007, **90**, 203113.
79 L. Pang, G. M. Hwang, B. Slutsky and Y. Fainman, *Appl. Phys. Lett.*, 2007, **91**, 123112.
80 M. E. Stewart, N. H. Mack, V. Malyarchuk, J. Soares, T. W. Lee, S. K. Gray, R. G. Nuzzo and J. A. Rogers, *Proc. Natl. Acad. Sci. U. S. A.*, 2006, **103**, 17143.
81 M. E. Stewart, J. M. Yao, J. Maria, S. K. Gray, J. A. Rogers and R. G. Nuzzo, *Anal. Chem.*, 2009, **81**, 5980.
82 F. Eftekhari, C. Escobedo, J. Ferreira, X. B. Duan, E. M. Girotto, A. G. Brolo, R. Gordon and D. Sinton, *Anal. Chem.*, 2009, **81**, 4308.
83 A. B. Dahlin, P. Jonsson, M. P. Jonsson, E. Schmid, Y. Zhou and F. Hook, *ACS Nano*, 2008, **2**, 2174.
84 J. R. Anema, A. G. Brolo, P. Marthandam and R. Gordon, *J. Phys. Chem. C*, 2008, **112**, 17051.
85 A. G. Brolo, E. Arctander, R. Gordon, B. Leathem and K. L. Kavanagh, *Nano Lett.*, 2004, **4**, 2015.
86 H. Wei, U. Hakanson, Z. L. Yang, F. Hook and H. X. Xu, *Small*, 2008, **4**, 1296.
87 S. Astilean, *Radiat. Phys. Chem.*, 2007, **76**, 436.
88 J. V. Coe, K. R. Rodriguez, S. Teeters-Kennedy, K. Cilwa, J. Heer, H. Tian and S. M. Williams, *J. Phys. Chem. C*, 2007, **111**, 17459.
89 K. Ide, M. Fujimoto, T. Kado and S. Hayase, *J. Electrochem. Soc.*, 2008, **155**, B645.
90 J. C. Johnson, T. H. Reilly, A. C. Kanarr and J. van de Lagemaat, *J. Phys. Chem. C*, 2009, **113**, 6871.
91 J. L. Skinner, A. A. Talin and D. A. Horsley, *J. Vac. Sci. Technol., B*, 2008, **26**, 2139.
92 J. L. Skinner, A. A. Talin and D. A. Horsley, *Opt. Express*, 2008, **16**, 3701.
93 T. Rindzevicius, Y. Alaverdyan, B. Sepulveda, T. Pakizeh, M. Kall, R. Hillenbrand, J. Aizpurua and F. J. G. de Abajo, *J. Phys. Chem. C*, 2007, **111**, 1207.
94 T. Rindzevicius, Y. Alaverdyan, M. Kall, W. A. Murray and W. L. Barnes, *J. Phys. Chem. C*, 2007, **111**, 11806.
95 S. P. Branagan and P. W. Bohn, *Opt. Express*, 2009, **17**, 18995.